HARD DIFFRACTION AT HERA

L.R.West
School of Physics and Space Research,
The University of Birmingham, Edgbaston,
Birmingham, B15 2TT, England

New results of diffractive phenomena observed at HERA are reported. The report focuses on the exclusive production of vector mesons, the deep inelastic structure of diffraction and complimentary information from diffractive final states.

1 Introduction

The HERA accelerator is the first ever electron-proton collider. It collides 27.5 GeV electrons (or positrons) against 820.0 GeV protons. Also, as the electrons radiate photons, HERA can also be thought of as a photon-proton collider.

One of the many interesting processes observed in the HERA data is that where a colouress object is exchanged. These events are referred to as 'diffractive', with the colourless exchange object termed the 'pomeron', $I\!P$, and can be compared to the predictions of the soft pomeron [1].

2 Kinematic Variables

The diffractive processes studied are of the form

$$e(k) + p(P) \rightarrow e'(k') + Y(P') + X \tag{1}$$

where Y can remain a proton and X can be a low-mass state or a vector meson. The relevant kinematic variables are $Q^2 = -q^2 = -(k-k')^2$, $t = (P-P')^2$ and $W^2 = (q+P)^2$ where q is the four momentum of the virtual photon and M_X (M_Y) the invariant mass of system X (Y). Variables used to describe the kinematics of the pomeron are

$$x_{I\!P} = \frac{(P-P')\cdot q}{P\cdot q} \simeq \frac{(Q^2+M_X^2)}{(Q^2+W^2)} \quad \text{and} \quad \beta = \frac{Q^2}{2(P-P')\cdot q} \simeq \frac{Q^2}{(Q^2+M_X^2)} \tag{2}$$

such that $x = x_{I\!P}\beta$.

The mass systems X and Y are separate due to the lack of colour flow between the proton and the photon. Hence, the event signature is a gap in rapidity between the two mass systems.

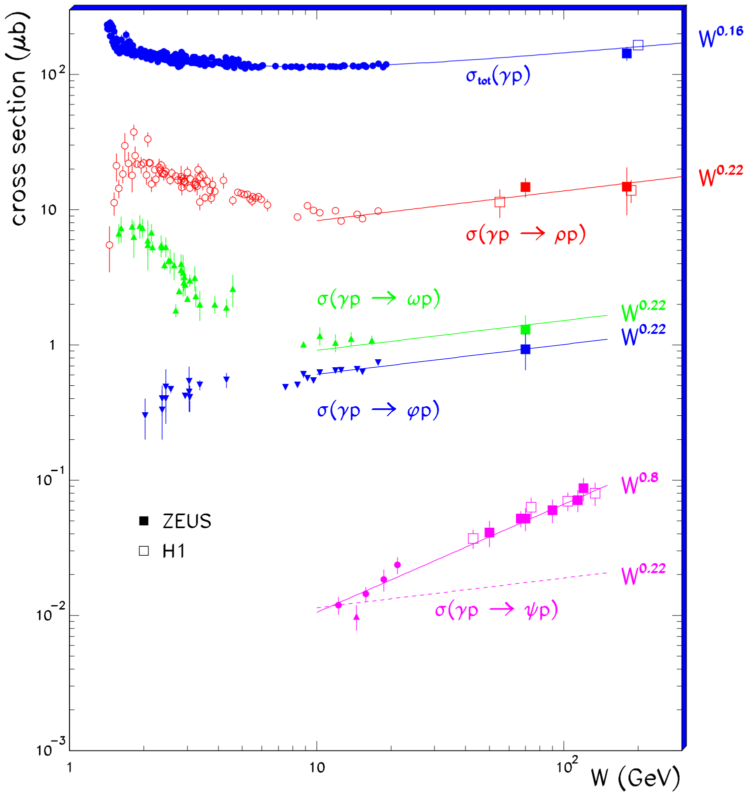

Figure 1: W dependence of the exclusive vector meson and total photoproduction cross sections compared to various power-law dependences.

3 Diffractive Vector Meson Production

Results have been obtained for vector meson production in photoproduction ($Q^2 \simeq 0$) and in deep inelastic scattering ($Q^2 > 4\,\mathrm{GeV}^2$).

The photoproduction cross sections for $\gamma p \to Vp$, when $V{=}\rho$, ω, ϕ or J/ψ, are shown in figure 1. Also shown is the total photoproduction cross section as this is related to the elastic, and hence diffractive, cross section by the optical theorem. The open and closed squares are results from H1 [2,3,4] and ZEUS [5,6,7,8] respectfully. All other symbols represent results from fixed target experiments.

The soft pomeron prediction for the total γp cross section, for large W, is $\sigma_{\gamma p} \propto W^{0.16}$ which is in very good agreement with the data. The cross section prediction for vector meson production, at large W, is $\sigma_{\gamma p \to V p} \propto W^{0.22}$ which again is in good agreement with the data when $V{=}\rho$, ω and ϕ. However, the W dependence of the J/ψ is much steeper ($\sigma \propto W^{0.8}$) than that predicted by the soft pomeron.

This steeper energy dependence is also seen in vector meson production at large Q^2 by both H1 [9] and ZEUS [10,11], when $V{=}\rho$, ϕ or J/ψ.

4 Cross Section for Diffractive Deep Inelastic Scattering

The differential $ep \to eXY$ cross section is related to the diffractive structure function, $F_2^{D(3)}$, by the equation (assuming $R = 0$)

$$\frac{\mathrm{d}^3\sigma^{\mathrm{D}}_{ep\to eXY}}{\mathrm{d}x_{I\!P}\,\mathrm{d}\beta\,\mathrm{d}Q^2} = \frac{4\pi\alpha^2}{\beta\,Q^4}(1 - y + \frac{y^2}{2})F_2^{D(3)}(\beta, Q^2, x_{I\!P}). \tag{3}$$

At present there are three different methods to measure $F_2^{D(3)}$.

4.1 Rapidity Gap Method

This method looks for large rapidity gap events [12,13] with the gap defined by measuring the maximum pseudo-rapidity of the most forward going particle (which must also be well away from the outgoing proton direction). An additional requirement is that there be no hadronic fragments (either primary or secondary) from Y in the forward detectors. This restricts M_Y to 1.4 and 4.0 GeV/c^2 for H1 and ZEUS respectively. This method has got the highest statistics due to the fact that the analysis has been done using both the 1993 and 1994 HERA data. The results for $F_2^{D(3)}$ can be seen in figure 2 as a function of $x_{I\!P}$ for different values of β and Q^2.

4.2 M_X Extrapolation Method

This method, which is only used by ZEUS [14], uses the M_X^2 distribution as a function of W. The probability of producing a gap for non-diffractive events is exponentially suppressed as a function of the rapidity gap and hence as a function of $ln(M_X^2)$. The diffractive data are observed as a low-mass shoulder to the M_X^2 distribution. Hence an exponential fit is made to the large M_X data to get an estimation of the non-diffractive signal. This fit is then used to subtract the number of non-diffractive events from the low M_X region.

The differential cross section $d\sigma^{\gamma^* p \to Xp}/dM_X \propto (W^2)^{2\overline{\alpha_{I\!P}}-2}$. The soft pomeron prediction for $\overline{\alpha_{I\!P}}$ is 1.05 whereas it is measured to be $1.23{\pm}0.02{\pm}0.04$

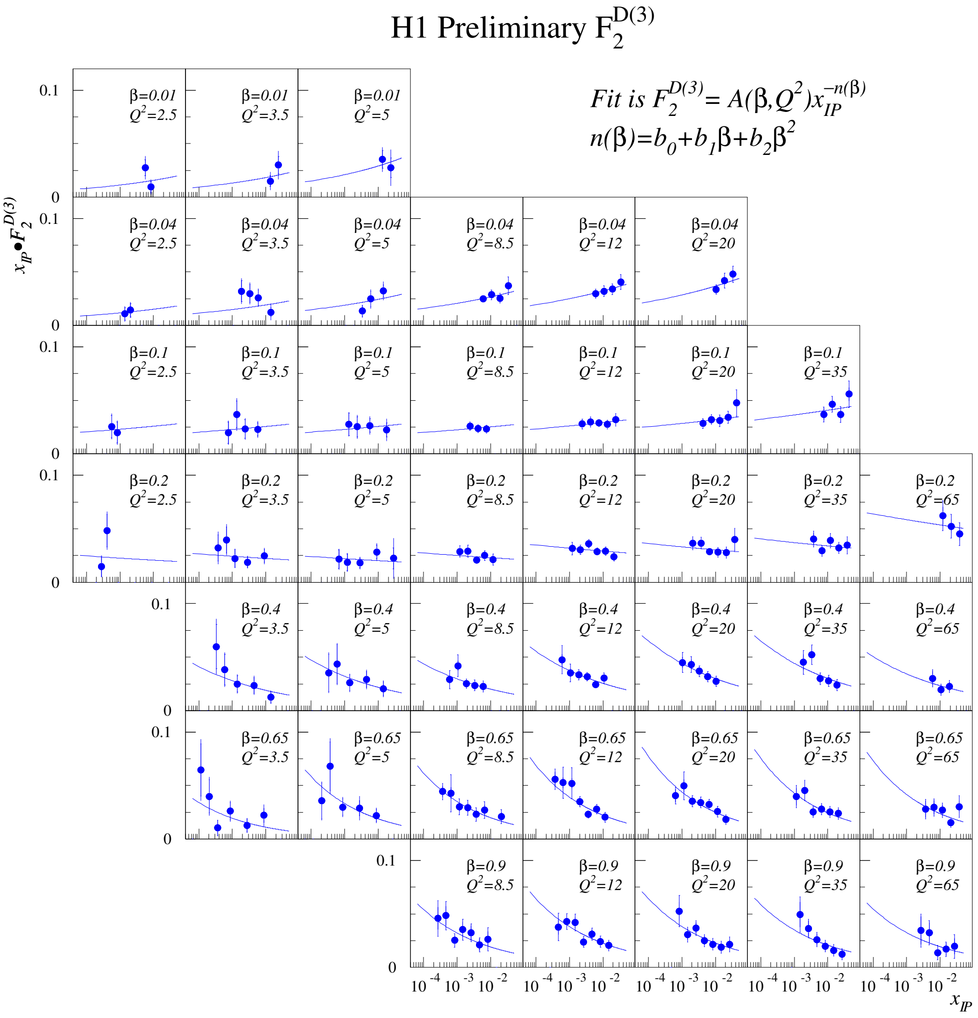

Figure 2: $x_{I\!P} \cdot F_2^{D(3)}(\beta, Q^2, x_{I\!P})$ together with a fit of the form $F_2^{D(3)} = A(\beta, Q^2)/x_{I\!P}^{n(\beta)}$. The experimental errors are statistical and systematic added in quadrature. The measurement is made for $0.0001 < x_{I\!P} < 0.05$, $0.01 < \beta < 0.9$ and $2.5 < Q^2 < 65$ GeV^2

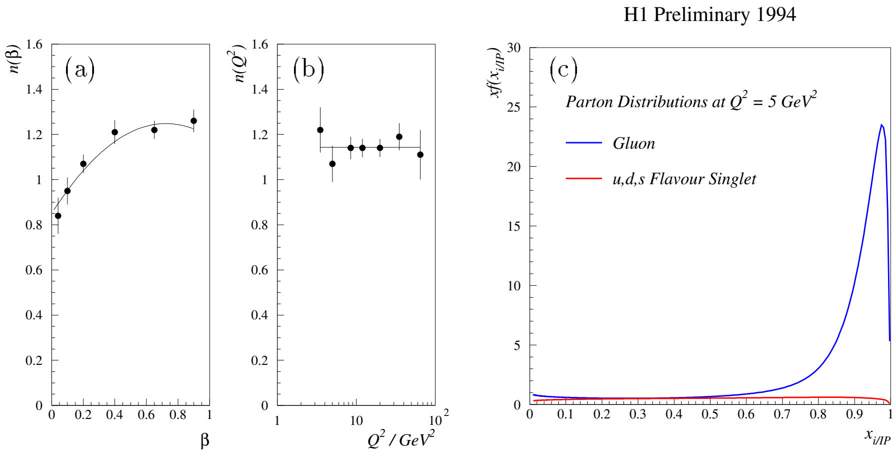

Figure 3: Plots of n as a function of (a) β and (b) Q^2 when testing factorisation and (c) the parton distributions for quarks and gluons of the QCD analysis.

in the data. So, as in section 3, a steeper energy dependence is observed in the data than that predicted by the soft pomeron.

4.3 The Leading-Proton-Spectrometer Method

The main advantage of this method is that the energy and angle of the scattered proton is measured and therefore t. The first ever t dependence in diffractive deep inelastic scattering has been measured using the 1994 ZEUS data. An exponential e^{-bt} is fitted to the data which yields a slope of $b = 5.9 \pm 1.2^{+1.1}_{-0.7}$. In the future it will be possible to make a measurement of $F_2^{D(4)}$.

5 Test of Factorisation

Factorisation is expected if the process of pomeron exchange and the interaction between the pomeron and the photon are independent. Factorisation requires that $F_2^{D(3)} = A(\beta, Q^2) \cdot f(x_{I\!P})$ where f is not a function of either β or Q^2. This is indeed tested using $f = 1/x_{I\!P}^n$ and from figure 3(b) it is seen that n is not a function of Q^2. However, from figure 3(a), n is found to be a function of β which is clear evidence of factorisation breaking. This non-factorisable fit of $F_2^{D(3)}$ can be seen in figure 2.

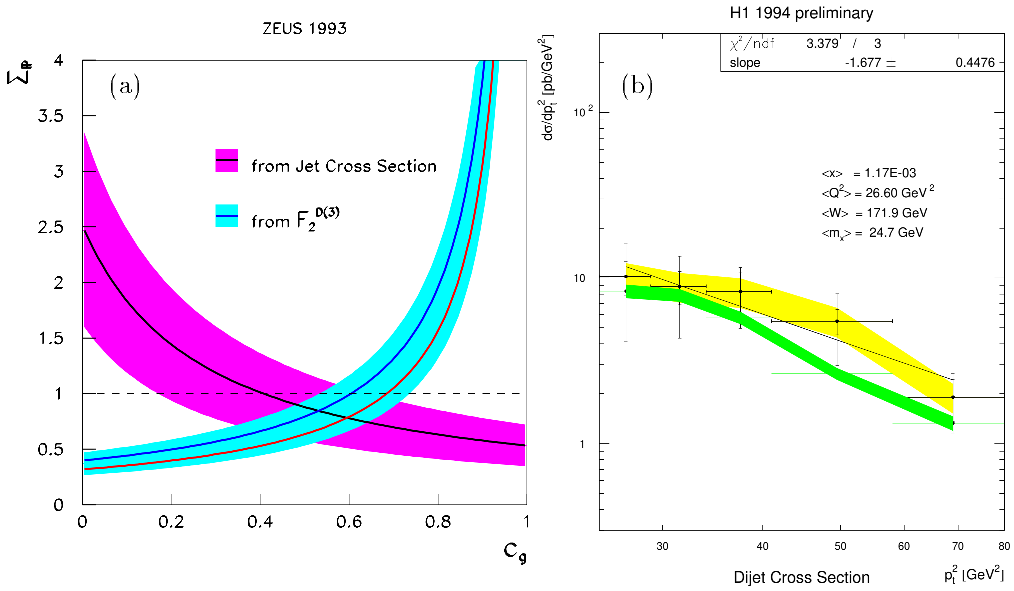

Figure 4: The plots show (a) the estimation of the gluon content using the overlap between photoproduction and deep inelastic diffractive inclusive jet cross section results and (b) the di-jets cross section (points) with the predictions from $\tilde{F}_2^{D(2)}$ (the lower shaded region).

6 The Partonic Structure of Diffractive Exchange

Integrating out the $x_{I\!P}$ dependence gives the pomeron structure function $\tilde{F}_2^{D(2)}$. A DGLAP [15,16] QCD analysis is performed with the result for the parton densities at $Q^2 = 5\,\mathrm{GeV}^2$ shown in figure 3(c). This analysis shows clear evidence for scaling violations, even to large values of β, and that a significant amount of the pomerons momentum is carried by gluons (80 % at $Q^2 = 5\,\mathrm{GeV}^2$).

7 Hadronic Final States

7.1 Inclusive Jet cross section

This uses the results from both the photoproduction and deep inelastic cross section measurements [17]. By varying the gluon content, a number of fits are made to the data. The results can be seen in figure 4(a). The overlap of the two fits give an estimate for the fraction of the pomerons momentum carried by gluons, which is found to be between 30 and 80 %.

7.2 Di-jets and Charm production

Using the QCD analysis of section 6, predictions for the di-jets and charm production rates can be estimated. The results for the di-jets cross section can be seen in figure 4(b) with the upper shaded region representing the calorimeter uncertainty. Only the predictions from $\tilde{F}_2^{D(2)}$ (the lower shaded region) is close to the measured cross sections. Using the decay channel $D^{*\pm} \rightarrow K^{\mp}\pi^{\pm}\pi^{\pm}_{slow}$, the prediction for charm production is also in good agreement with the data.

8 Conclusions

The soft pomeron can predict the cross sections for vector meson photoproduction when the vector meson is either a ρ, ω or ϕ. However, this is not the case for the photoproduced J/ψ and deep inelastic vector meson production where a steeper energy dependence is observed. This steep energy dependence is also seen in the deep inelastic diffractive scattering data. Further studies of the diffractive exchange suggest that factorisation is broken, scaling violations are observed and that a significant fraction of the pomerons momentum is carried by gluons. These observations are confirmed from the studies of the diffractive final states.

References

1. A. Donnachie and P. Landshoff, *Nucl. Phys.* B **244**, 322 (1984).
2. H1 collaboration, S. Aid *et al*, *Z. Phys.* C **69**, 27 (1995).
3. H1 collaboration, S. Aid *et al*, *Nucl. Phys.* B **463**, 3 (1996).
4. H1 collaboration, S. Aid *et al*, DESY preprint **96-037**, (1996).
5. ZEUS collaboration, M. Derrick *et al*, *Z. Phys.* C **63**, 391 (1994).
6. ZEUS collaboration, M. Derrick *et al*, DESY preprint **95-143**, (1995).
7. ZEUS collaboration, M. Derrick *et al*, DESY preprint **96-002**, (1996).
8. ZEUS collaboration, M. Derrick *et al*, *Phys. Lett.* B **350**, 120 (1995).
9. H1 collaboration, S. Aid *et al*, DESY preprint **96-023**, (1996).
10. ZEUS collaboration, M. Derrick *et al*, *Phys. Lett.* B **356**, 601 (1995).
11. ZEUS collaboration, M. Derrick *et al*, DESY preprint **96-067**, (1996).
12. H1 collaboration, T. Ahmed *et al*, *Phys. Lett.* B **348**, 681 (1995).
13. ZEUS collaboration, M. Derrick *et al*, *Z. Phys.* C **68**, 569 (1995).
14. ZEUS collaboration, M. Derrick *et al*, *Z. Phys.* C **70**, 391 (1995).
15. V. N. Gribov and L. N. Lipatov, *Sov. Journ. Nucl. Phys.* **15**, 78 (1972).
16. G. Altarelli and G. Paraisi, *Nucl. Phys.* B **126**, 298 (1977).
17. ZEUS collaboration, M. Derrick *et al*, *Phys. Lett.* B **356**, 129 (1995).